Batteries & Supercaps

Minireviews
doi.org/10.1002/batt.202100174

Chemistry Europe
European Chemical Societies Publishing

www.batteries-supercaps.org

VIP *Very Important Paper*

Synthesis and Processing by Design of High-Nickel Cathode Materials

Feng Wang*[a] and Jianming Bai*[a]

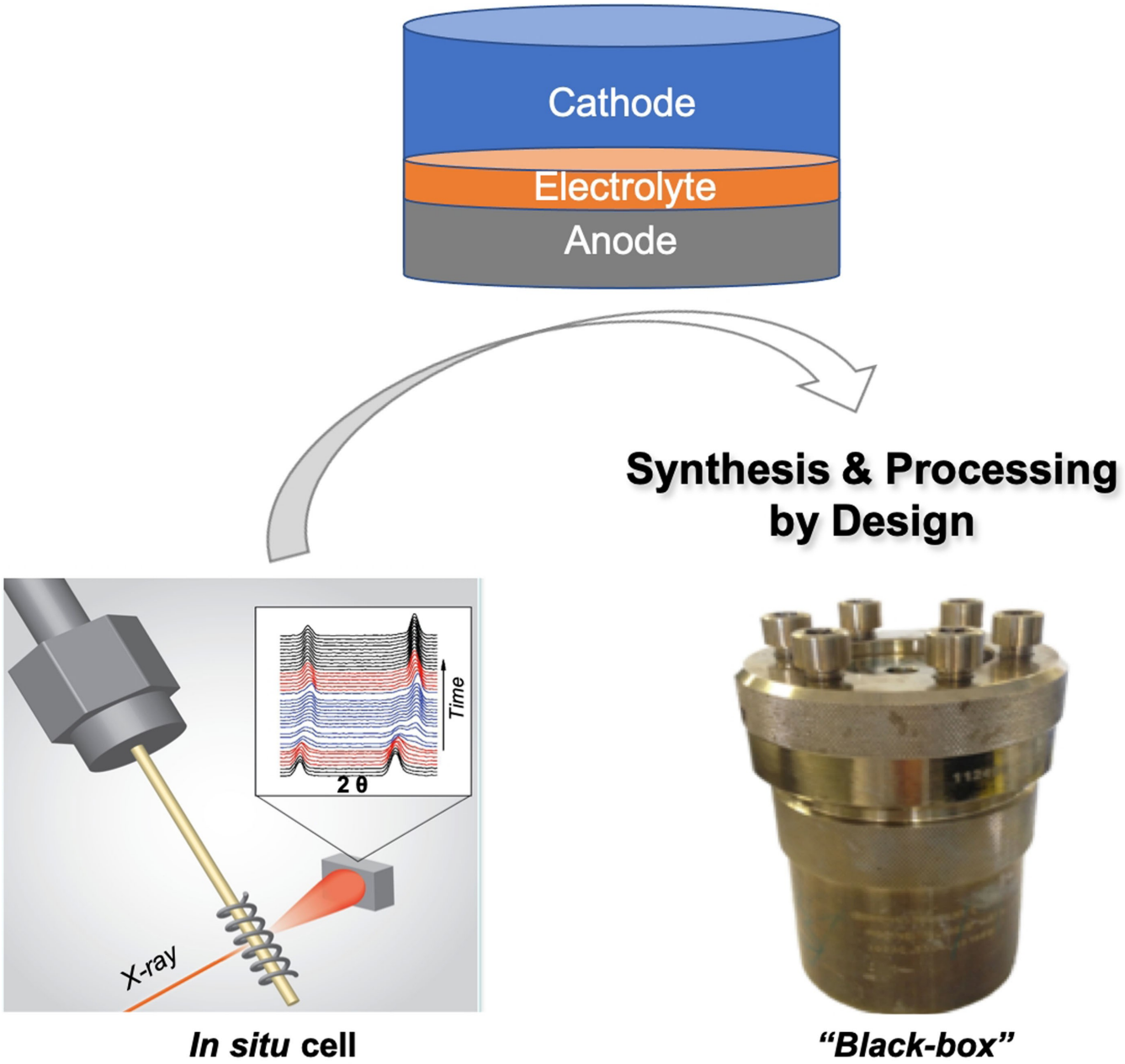

The high demand of lightweight, high energy density batteries for energy storage promotes new materials discovery and development. Despite the large number of battery materials being discovered, very few of them have been commercially deployed, mostly bottlenecked by synthesis and processing – namely, making certain phases with the desired structure and properties to meet the multifaceted performance requirements. Alternative to the traditional *trial and error*, we present here an in situ study aided *synthesis- and processing-by-design* approach. With specific examples, we illustrate how to use the approach to identify reaction pathways in synthesis and processing of high-Nickel (Ni) cathode materials for next-generation lithium-ion batteries, thereby ensuring precise control of their structure, morphology, and surface properties. To the end, perspectives are provided on the wide applicability of the approach to solving critical issues inherent to high-Ni cathodes and the new directions and opportunities in the area.

1. Introduction

Lithium-ion battery (LIB) is now the dominant power source for portable electronic devices and increasingly used for electric vehicles (EVs) and other large-scale applications due to its high energy density and long life span.[1,2] Similar to other types of batteries, a Li-ion based battery system is first of all an electrochemical device, or chemical-electrical energy converter comprising multiple parallel- or series-connected cells. Each cell, at a fundamental level, consists of an anode, electrolyte, and cathode. During the charge/discharge operation of LIBs, Li ions move back and forth between anode and cathode (through the electrolyte). An important parameter of performance for LIBs is the specific or volumetric energy density, which is determined by the specific capacity of the anode and cathode (namely the amount of Li ions that can be stored per unit weight or volume) and the difference of electrochemical potentials between the two elecrodes (anode and cathode).

The first-generation LIBs commercialized by Sony Corporation were based on hard carbon as anode and lithium cobalt oxide ($LiCoO_2$; LCO) as cathode. Thereafter, graphite (Gr) was introduced to replace carbon, for its flat working potential, high capacity (~ 370 mAh/g). Additionally and importantly, Gr electrodes exhibit high stability in non-aqueous electrolyte via forming an interfacial layer, the so-called solid-electrolyte interphase. Over the past several decades, a number of anodes and cathodes have been developed and employed throughout the history of LIBs, from the first/second-generation, to the *state-of-the-art* and to the next generation (Figure 1). Even today, Gr/LCO-based cells still attract high commercial interest, while cells comprising $Li_4Ti_5O_{12}$ or Si-based anodes have recently been commercialized, being preferred over other alternatives for meeting specific safety or energy density requirements in certain applications.

LIBs are the power sources of choice for portable electronics, but one bottleneck for large-scale applications has been the low Li-storage capacity, largely constrained by the cathode side, typically with a gravimetric capacity equivalent to ~ $^1/_2$ of the Gr anode. Due to the low capacity and high cost of LCO, among other issues that limit its use in EVs and other large-scale applications, alternatives, such as spinel ($LiMn_2O_4$) and olivine ($LiFePO_4$) were developed.[3] They are favorable for many applications due to their long life span and low cost, but have the disadvantage of low specific energy density, particularly for the use in EVs.[4] Over the past decades, there has been intense effort on developing new cathode materials with higher specific capacity and/or higher working potential, leading to the discovery of many seemingly promising cathode materials. So far, very few of them have been synthesized, and even fewer have realized their full capacity.[5]

In the early search of alternatives to LCO cathodes, $LiNiO_2$ (LNO) attracted great attention because of its isostructural characteristics, lower cost and higher practical capacity (above 200 mAh/g). However, stoichiometric LNO is hard to synthesize, and its thermal instability at high states-of-charge (SOC) has been a safety concern. Different strategies were developed to mitigate these issues and among them, elemental substitution has been shown most effective by adding a second and even third cation into the transition metal (TM) layers to construct solid solutions. For example, Co is added into $Li[Ni_x(TM)_{1-x}]O_2$ in conjunction with Al or Mn to form $LiNi_{0.8}Co_{0.15}Al_{0.05}O_2$ or $LiNi_{1/3}Mn_{1/3}Co_{1/3}O_2$, wherein Co helps to improve structural ordering, and Al or Mn to strengthen thermal stability, leading to the commercial use of such type of cathodes in the second generation of LIBs.[6]

1.1. Next-Generation Cathode Materials

Li/Mn-rich layered oxides ($xLi_2MnO_3{\cdot}(1\text{-}x)LiMO_2$; M = Mn, Ni, Co) are attractive cathode materials with extremely high capacity (up to 300 mAh/g), low cost, and high thermal stability.[7,8] Experimental and first principles studies demonstrated that excess capacity may come from oxygen redox reaction, additional to that from cationic redox.[9,10] However, these cathode materials exhibit critical drawbacks such as voltage fade in association with voltage hysteresis, low first-cycle efficiency, and low rate capability, therefore limiting practical applications.[8,11] Extensive research has been conducted to develop strategies for tuning the kinetics and reversibility of the oxygen redox reaction, aiming at improving the energy efficiency and cyclability of such cathodes. [12,13] Incorporation of a lithiated spinel component has been demonstrated to be promising in improving the stability against TM migration and

[a] *Dr. F. Wang, Dr. J. Bai*
Energy and Photon Sciences Directorate
Brookhaven National Laboratory
Upton, New York 11973, USA
E-mail: fwang@bnl.gov
jmbai@bnl.gov

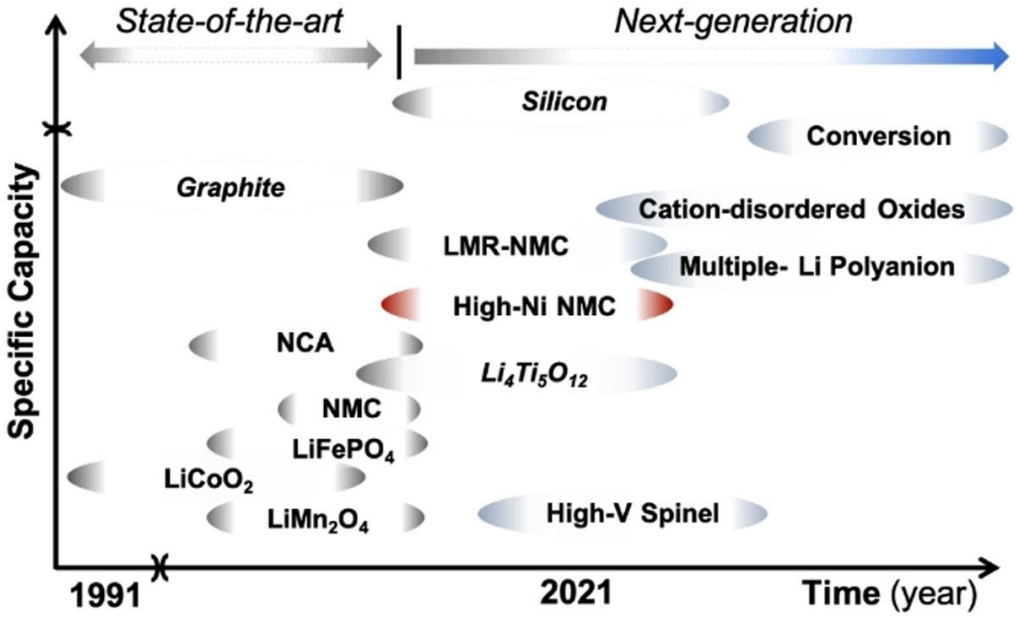

Figure 1. Roadmap of the development of anode and cathode materials for commerical deployment in the 1st generation, state-of-the-art, and next-generation LIBs.

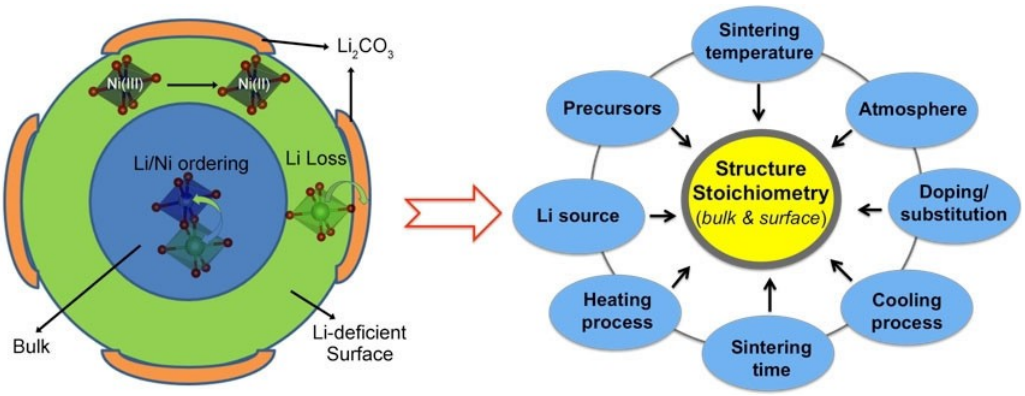

Figure 2. Schematic of the issues associated with capacity fading in high-Ni cathodes, such as structural disordering and surface reconstruction (as illustrated on the left), which may be addressed by synthesis and processing with an intended control of the structure/stoichiometry in the bulk and surface via tuning synthesis/processing parameters (as listed on the right).

battling against the first-cycle capacity loss.[14] However, mitigation of the voltage fade remains challenging, especially in the presence of excess Li and Mn. Moreover, synthetic control of the stoichiometry and structural properties of Li/Mn-rich layered oxides using the conventional solid-state reaction methods has been challenging.

Feng Wang is a materials scientist at Brookhaven National Laboratory. He obtained his Ph.D. in condensed matter physics from the University of Alberta. His research has centered on advancing electron microscopy and synchrotron X-ray techniques as applied to materials design, synthesis, and characterization. He is presently a Principal Investigator leading multiple projects ranging from fundamental research to applied battery technologies for electric vehicles and other large-scale applications.

Jianming Bai is a beamline scientist at the National Synchrotron Light Source II. He completed B.S. and M.S. in Physics from Peking University and Ph.D. from City University of New York. He has been working for more than 20 years in the development of synchrotron X-rays instruments and methods for materials characterization. His current research interest is on in situ synchrotron X-ray studies on processes in materials synthesis.

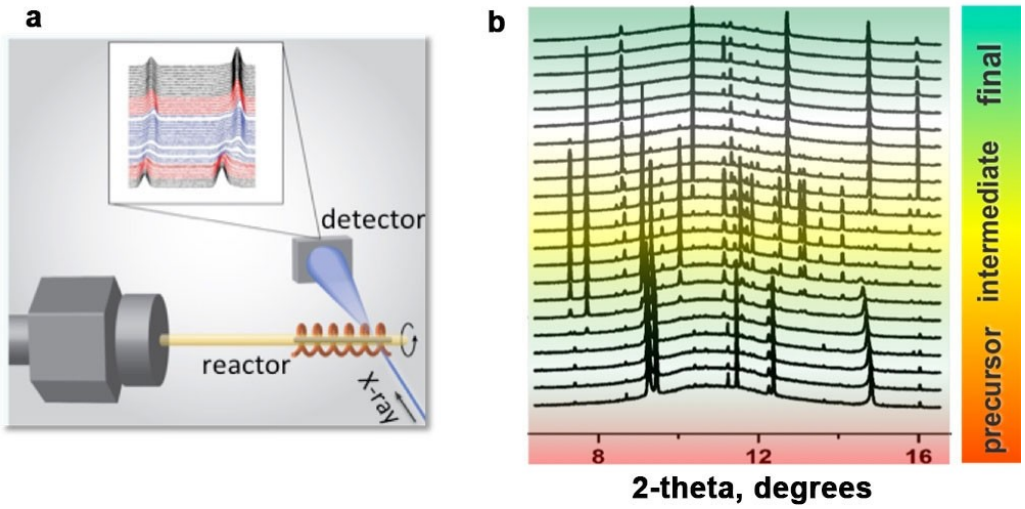

Figure 3. In situ synchrotron XRD studies of synthesis of $LiFePO_4$ via solvothermal process. a) Illustration of the setup. b) Temperature-resolved XRD patterns acquired throughout the synthesis process, from precursors, intermediates and the final product (color coded). (Adapted with permission from Ref. [32]. Copyright (2015) American Chemical Society)

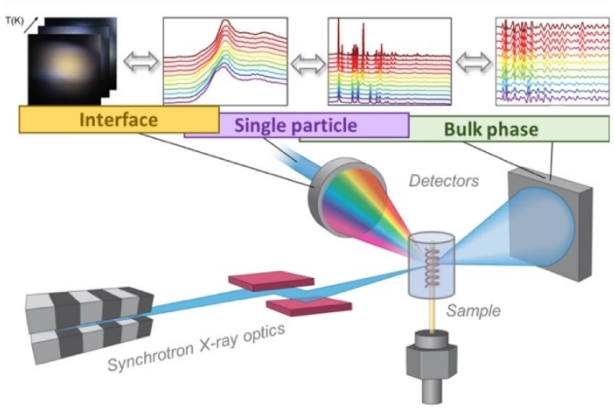

Figure 4. Schematic illustration of the experimental setup for in situ synchrotron X-ray multimodal characterization of the reactions and processes involved in the synthesis and processing of battery materials, at scales varying from the bulk phase to single particles and interfaces.

Cation-disordered oxides (Li–M-O_2; M = Mn, Nb, Mo, Ti, Fe, …) are an appealing alterative of high-capacity layered cathodes that exhibit a rocksalt-like structure with partial or complete cationic disordering.[15] In the traditional layered oxides, a high cationic ordering is necessary to realize high Li diffusivity; however, the restrictive requirement becomes no longer applicable to cation-disordered oxides. A percolation network of "0-TM" channels to facilitate Li diffusion can be created using approximately 10% excess Li in such cation-disordered oxides. This opens a new avenue for making high-capacity cathodes from nontypical metallic elements, thereby ensuring economization of both resources and cost.[16,17] Cation-disordered oxides are also dimensionally stable with low volume expansion, which is necessary to achieve long-term, safe operations. Such cathode materials are still in their early stage of development and much needs to be done on material optimization (i.e., composition, structure) to ensure optimal energy density, lifespan, and rate performance.

Nickel (Ni)-based layered oxides ($Li[Ni_x(MnCo)_{1-x}]O_2$; NMC), such as NMC622 and other Ni-rich NMCs ($x \geq 0.5$), have become commercially available; high-Ni ($x \geq 0.8$) and low-Co NMCs are now the most intensely pursued cathode materials owing to their high capacity and low cost.[18,19] Unfortunately, high-Ni loading brings the inherent surface-instability issue and, consequently, the compromised cyclability and safety.[20] Surface instability is also a problem for material production/storage and electrode fabrication, posing a significant obstacle to the commercial deployment of these cathode materials.[16]

1.2. Challenges in Developing High-Ni Cathodes

To enable commercial application of high-Ni cathodes, strategies are needed to manage the competing factors of high Ni loading. High output capacity requires high Ni content; but as Ni content increases, Ni sitting at octahedra tends to go to Li sites in the crystal lattice, resulting in reduced electrochemical activity.[21] Cathodes are generally charged to high voltages (above 4.2 V) to achieve high energy density, meanwhile introducing a number of mechanical issues such as cracking due to lattice collapse, gas release, structural reconstruction (or surface densification). Such undesired phenomena may happen concomitantly and, consequently, lead to poor cyclability and voltage decay, which has been a main obstacle to the realization of high-Ni NMCs with true commercial potential.[22,23] Eventually, addressing such issues relies on synthesis and processing, in obtaining the materials with controlled structure and stoichiometry, not only in the bulk, but also at the surface (see Figure 2 using an example on solid-state synthesis). In particular, Li is readily lost from the surface during high-temperature heat treatment, leading to a Li-deficient layer and, in the extreme, formation of electrochemically inactive

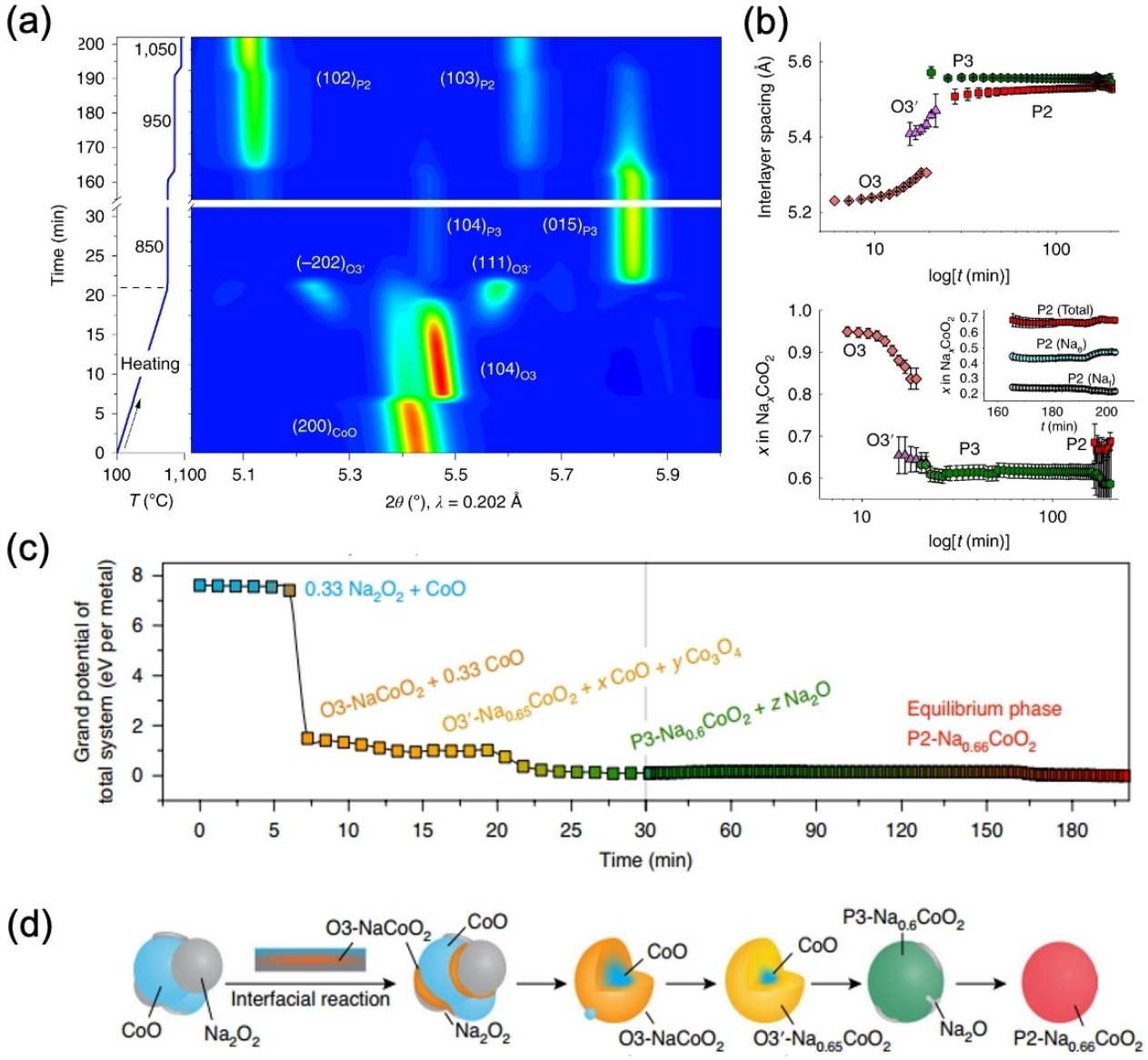

Figure 5. a) Evolution of the grand potential for the total system in the reaction vessel, normalized by the number of metal cations (Na, Co). Two different scales are used on the time axis to highlight the multiple phase transitions in the initial 30 min. b) Schematic of the reaction pathway via interfacial reactions. c) Evolution of the grand potential open to an external oxygen reservoir, for the total system in the reaction vessel, normalized by the number of metal cations (Na, Co). Two different scales are used on the time axis to highlight the multiple phase transitions in the first 30 min. d) Cartoon suggesting a physical model of the reaction pathway via interfacial reactions. (Adapted with permission from Ref. [48]. Copyright (2020) The Author(s), under exclusive license to Springer Nature Limited)

rocksalt.[24] It has been shown that surface species, such as Li_2CO_3, react with electrolyte, leading to gassing, as exampled by the CO and CO_2 release during the charging/discharging process.[25]

Some of these issues may be mitigated by doping, surface coating or synthesis of particles with core-shell or concentration-gradient structures.[26–28] However, the implementation of these strategies for large-scale production is inhibited by the complexity associated with the processing/synthesis, in obtaining the high-Ni cathode materials with the desired compositional heterogeneity and structural ordering .[29,30] In principle, electrode performance, which is largely determined by the structural properties of active materials, can be advanced through synthesis/processing.[31] But practically, the reactions and processes invoved in synthesis/processing are complex and highly sensitive to various parameters such as temperature, reaction time, pressure, pH, and cation type/concentration in the precursors. In addition, synthesis and processing are mostly undertaken under non-equilibrium conditions, making it hard to predict the reaction pathways by theories or computations. Making cathode materials of desired structure and properties has been a non-trivial task and becomes even more challenging for the specific system of high-Ni NMC oxides due to the Li/Ni mixing, surface instability. Additional challenge comes from the chemical and spatial inhomogeneity in the oxidation states

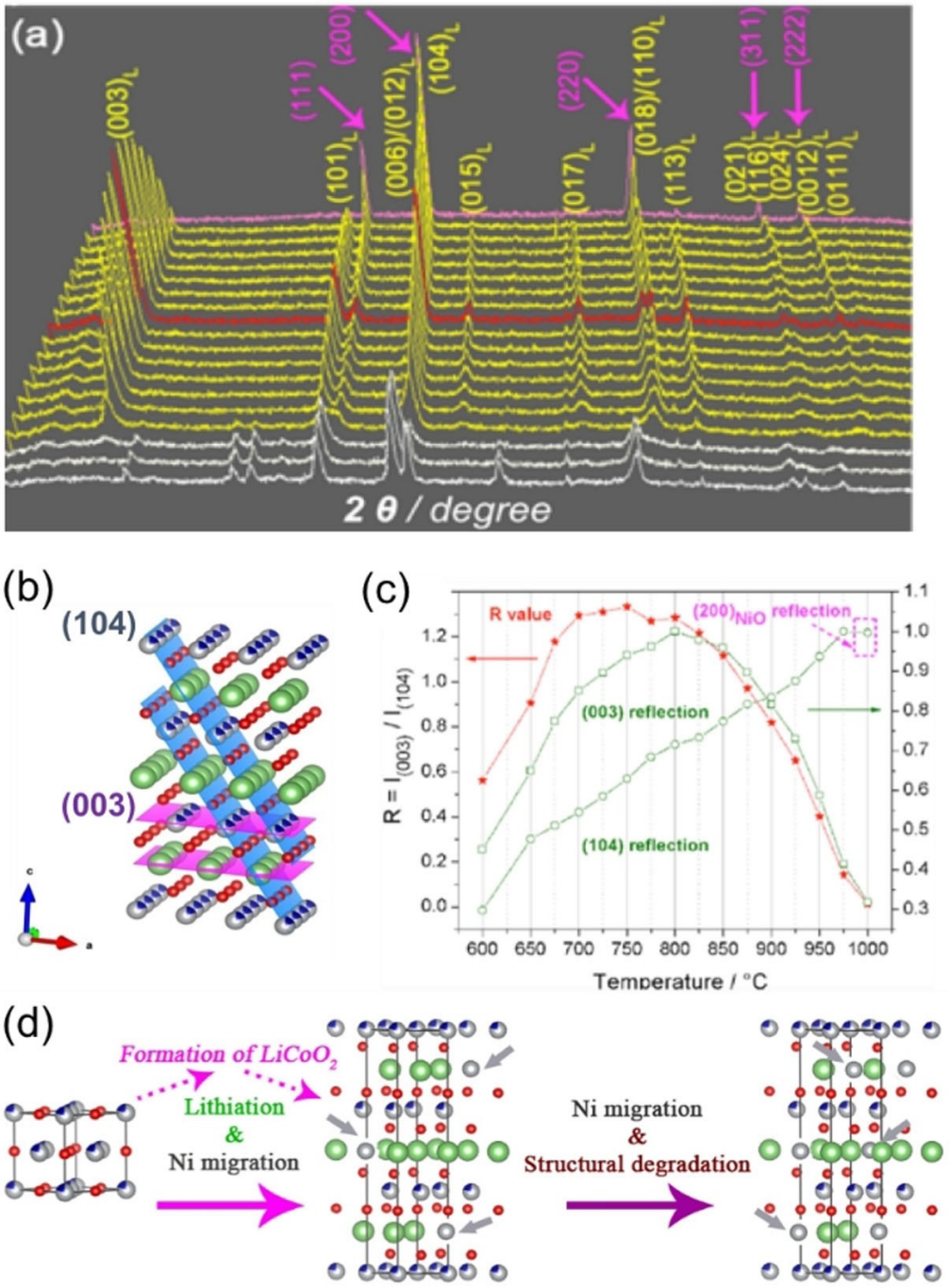

Figure 6. In situ studies of the process in synthesis of Ni-based layered oxides under an O_2 flow. a) Representative temperature-resolved XRD patterns recorded during synthesis of $LiNi_{0.8}Co_{0.2}O_2$. b) Schematic of the atomic configuration and reflection planes ((104) and (003)) in the layered structure. The (003) reflection is highly sensitive to the cationic ordering (i.e., occupancies of Li, Ni, and Co youions), whereas the (104) reflection is independent of the cationic ordering. c) Evolution of the intensity ratio of the (003) and (104) reflections ($R = I(003)/I(104)$). d) Schematic of the local cation migration, ordering and related structural evolutions, directly from rocksalt to the layered phase during synthesis of $LiNi_{0.8}Co_{0.2}O_2$. Adapted with permission from Ref. [29]. Copyright (2016) Wiley-VCH.

across individual particles and the dynamical evolution caused by elemental inter-diffusion, segregation, and Li/O loss.[23,25]

We present here a structure tracking-aided synthesis-/processing-by-design approach, using in situ techniques for real-time tracking of the reactions/processes during materials synthesis/processing, both in the bulk and individual particles, down to surface/interfaces. Quantitative data analysis is applied to identify the details of structural evolution in the involved intermediates and, in conjunction with theoretical calculations, to gain insights into the reaction kinetics/thermodynamics and underlying mechanisms. With specific examples from recent studies, we show how to apply the approach to elucidate the reaction pathways in synthesis/processing of high-Ni cathode materials, thereby enabling precise control of their structure,

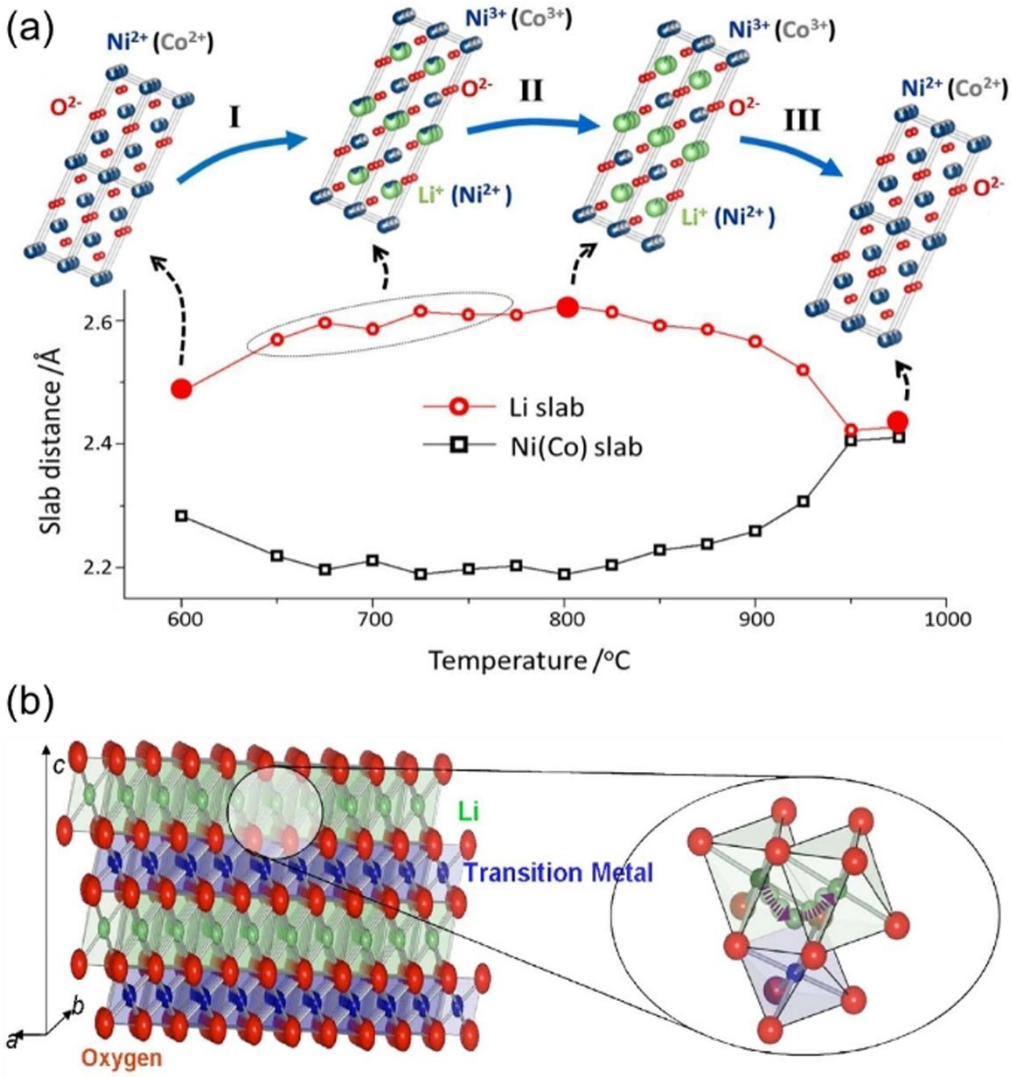

Figure 7. Insight into synthetic control of the structural and electrochemical properties of layered oxides. a) Evolution of the Li and Ni(Co) slab distances as a function of temperature along with detailed structural evolution in the intermediates (top) during synthesis of the layered $LiNi_{0.8}Co_{0.2}O_2$. Adapted with permission from Ref. [29]. Copyright (2016) Wiley-VCH. b) Schematic of Li hops between octahedral sites through an intermediate tetrahedral site in layered lithium TM oxides, indicating the high sensitivity of the Li diffusivity to the Li slab distance. Adapted with permission from Ref. [53]. Copyright (2006) American Physical Society.

morphology, and surface properties. Perspectives are provided on the wide applicability of the approach to alleviating some of the critical issues pertaining in high-Ni cathode materials, such as cationic disordering and surface reconstruction among others. New directions and opportunities in the area will be discussed to the end.

2. Approach: Synthesis/Processing-by-Design

Alternative to the traditional *trials and errors*, materials synthesis and processing may be rationally designed with the insights from *in situ* studies. Specifically, *in situ* techniques are developed for real-time probing of the intermediate phases and their structural evolution as the materials are being synthesized/processed. This allows access to the details of the processes, elucidating how the synthesis/processing parameters affect the kinetics and reaction pathways. Such studies, with the insights into the reaction process and the involved intermediates under real conditions, provide a basis for materials synthesis/processing by design – rationally selecting synthesis/processing parameters to improve performance and reduce cost.

2.1. Techniques for In Situ Probing of Synthesis/Processing

X-ray/neutron diffraction has been commonly used for materials characterization and is arguably the most powerful tool among various scattering and spectroscopy techniques for in situ characterization of synthesis/processing reactions. Since most of battery materials are in the polycrystalline form,

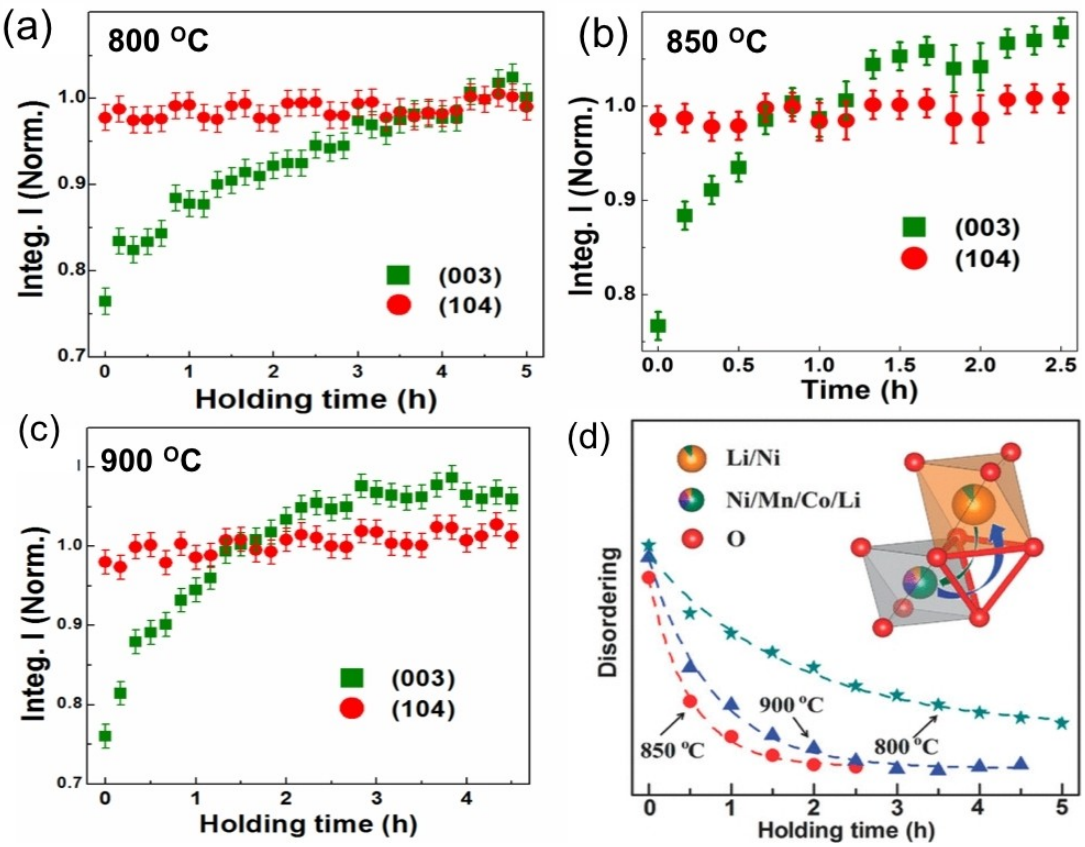

Figure 8. In situ tracking of structural ordering in the intermediates during synthesis of NMC71515. a)-c) Evolution of the integrated intensity of the (003) and (104) reflections during heat treatment at temperatures 800 °C, 850 °C, 900 °C, respectively. d) Strong dependence of the cationic disordering (i.e., Ni ions at Li (3b) sites; inset) on temperatures. Adapted with permission from Ref. [54]. Copyright (2017) Wiley-VCH.

powder diffraction is commonly employed for monitoring the structural evolution during synthesis/processing. Advanced synchrotron facilities provide powerful powder diffraction capability that allows following the reactions and processes with high precision and in short time. As demonstrated by the early studies on hydrothermal/solvothermal and solid-state synthesis of $LiFePO_4$, in situ synchrotron XRD is capable of resolving the involved intermediates, including minor impurity phases and their structural evolution under the real synthesis conditions (Figure 3).[32,33,34]

Over the years, various in situ techniques have been developed for studying synthesis/processing reactions. With the special design of sample configuration and environment, one same sample may be loaded into different beamlines/facilities for complementary characterization using multiple in situ techniques, such as x-ray fluorescence imaging, x-ray absorption spectroscopy (XAS), XRD, and x-ray total scattering coupled with pair distribution function (PDF) analysis (as illustrated in Figure 4). Results from such multimodal characterization, covering both bulk measurements with a large volume of materials being sampled and local probing of structural/chemical evolution in heterogeneous materials and at surfaces/interfaces, provide a science basis for the rational design of materials synthesis/processing.

2.2. Quantitative Analysis and Modeling Coupled with In Situ Characterization

Synchrotron X-ray techniques, especially those based on XRD are suited for in situ probing of phase evolution during synthesis/processing, but to tackle the complexity and mechanisms of the involved reactions/processes, quantitative analysis and modelling often become crucial. The quantitative analysis of powder diffraction data often starts with structural modelling, by assigning parameters representing the unit cell dimension, atomic position and occupancy, micro-strain and crystalline sizes, phase composition, etc.; in addition, space groups are utilized to describe the structural symmetry of each phase. The XRD pattern can be calculated based on the model and compared with experimental data via Rietveld refinement, a process to minimize the difference.[35]

First-principles calculations based on the density-functional theory (DFT) have frequently been adopted to predict stable crystal structure of compounds by identifying the lowest energy or free energy of the electronic systems.[36] The quantitative data analysis in conjunction with DFT calculation provide a detailed understanding of the stability of structures.[37] In general, the DFT calculated structure model can be used as a starting point for XRD analysis, and/or to calculate a formation-energy convex hull from a series of structural

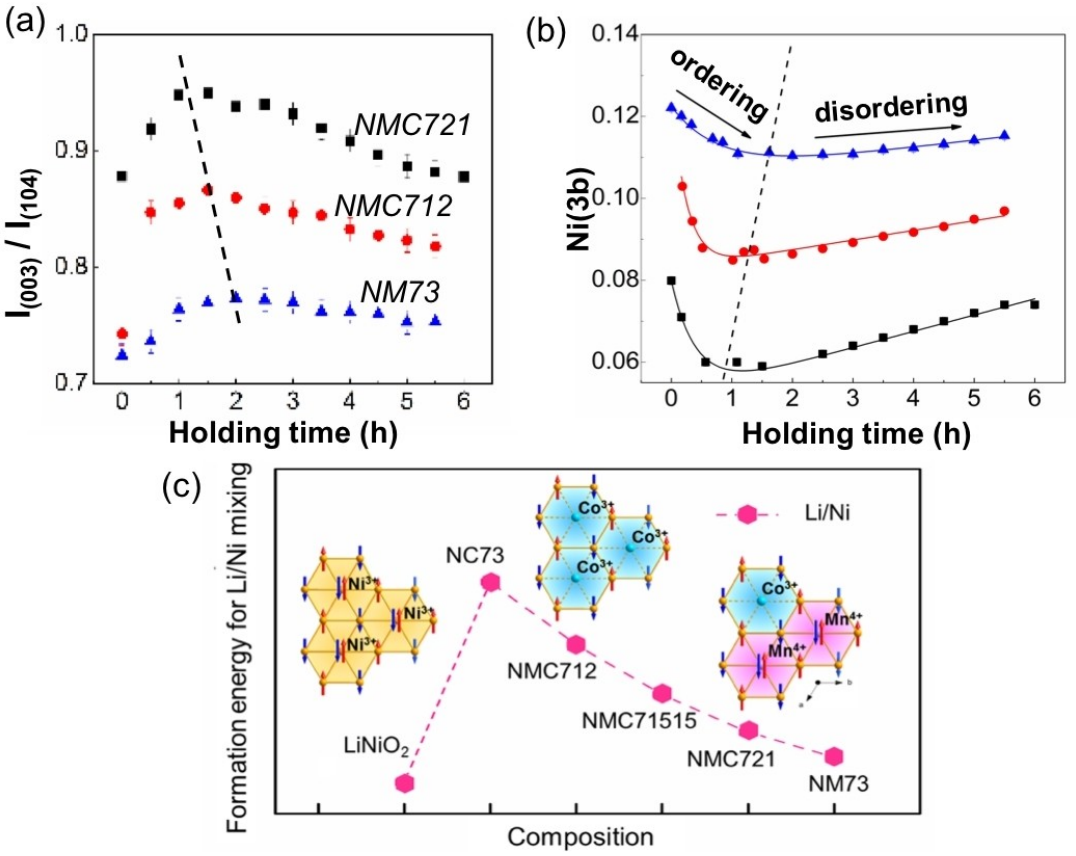

Figure 9. Role of Mn/Co substitution in tuning the cationic ordering/disordering in $LiNi_{0.7}Mn_xCo_{0.3-x}O_2$ ($0 \leq x \leq 0.3$). a, b) Similar trend of change in the $I_{(003)}/I_{(104)}$ ratio and Li/Ni disordering as a function of time but strong compositional dependence of the ordering/disordering kinetics. c) Formation energy for Li/Ni mixing as a function of the composition. Adapted with permission from Ref. [55]. Copyright (2019) American Chemical Society.

configurations to verify whether the structure derived from XRD measurements is the most stable phase, i.e., the lowest-energy configuration.[38,39]

There are a few empirical models or classical thermodynamic based rationalization of the reaction pathway and kinetics. The Ostwald's Rule states that in a crystallization process, the first crystallized phase will be the one of least stable, with the highest Gibbs free energy.[40] Avrami equation describes the kinetics of a nucleation-growth-saturation process,[41] and was used, for example, to characterize the crystallization of the $LiFePO_4$ in a hydrothermal synthesis.[33] The Arrhenius equation is used for calculating the temperature dependence of reaction rate,[42] and often utilized to estimate the activation energy of synthesis reactions.[43]

In synthesis/processing of Li-ion battery materials, migration of cations (both Li and TM ions) is an important process. Their mobility and migration pathways are critical parts of the reaction mechanisms and can be predicted with the nudged elastic band (NEB) method.[44] The NEB algorithm finds the minimum energy path of migrating ions between two structural configurations, which may be determined by in situ XRD analysis.[45] Bond valence sum (BVS) is widely used in coordination chemistry to estimate the valences of cations. It describes an empirical relationship between bond length and the bond valence based on accumulated experimental data.[46] It is also frequently used to validate newly determined crystal structures and assess the ionic conduction paths from the knowledge of the crystal structure. For example, Li-ion and Na-ion mobilities in the lattice structures of $Li_2Mg_2P_3O_9N$ and $Na_2Mg_2P_3O_9N$ were estimated by examining the percolation thresholds in the BVS difference maps.[47]

In a recent study, a theoretical framework was developed based on ab initio thermodynamics to rationalize the multistep crystallization pathways in a solid-state synthesis of layered sodium oxide $Na_{0.67}MO_2$ (M = Co, Mn), being observed from in situ XRD measurements (Figure 5a, b).[48] As the grand potential changes as a function of time, the first metastable intermediate should have consumed the major portion of the total reaction free energy (Figure 5c), likely via interfacial reactions among many possible pathways (Figure 5d). The combined theoretical and in situ studies show that the local composition at the interfaces of precursors can be different to the overall composition, leading to the formation of the intermediate phase with the local minimum, namely, the interfaces with the most negative reaction free energy. In other words, it is the local composition that sets the preference of the first crystallized phase, being observed from in situ XRD measurements (Figure 5a, b).

The developed approaches have been applied for structure-tracking aided synthesis of different types of cathode

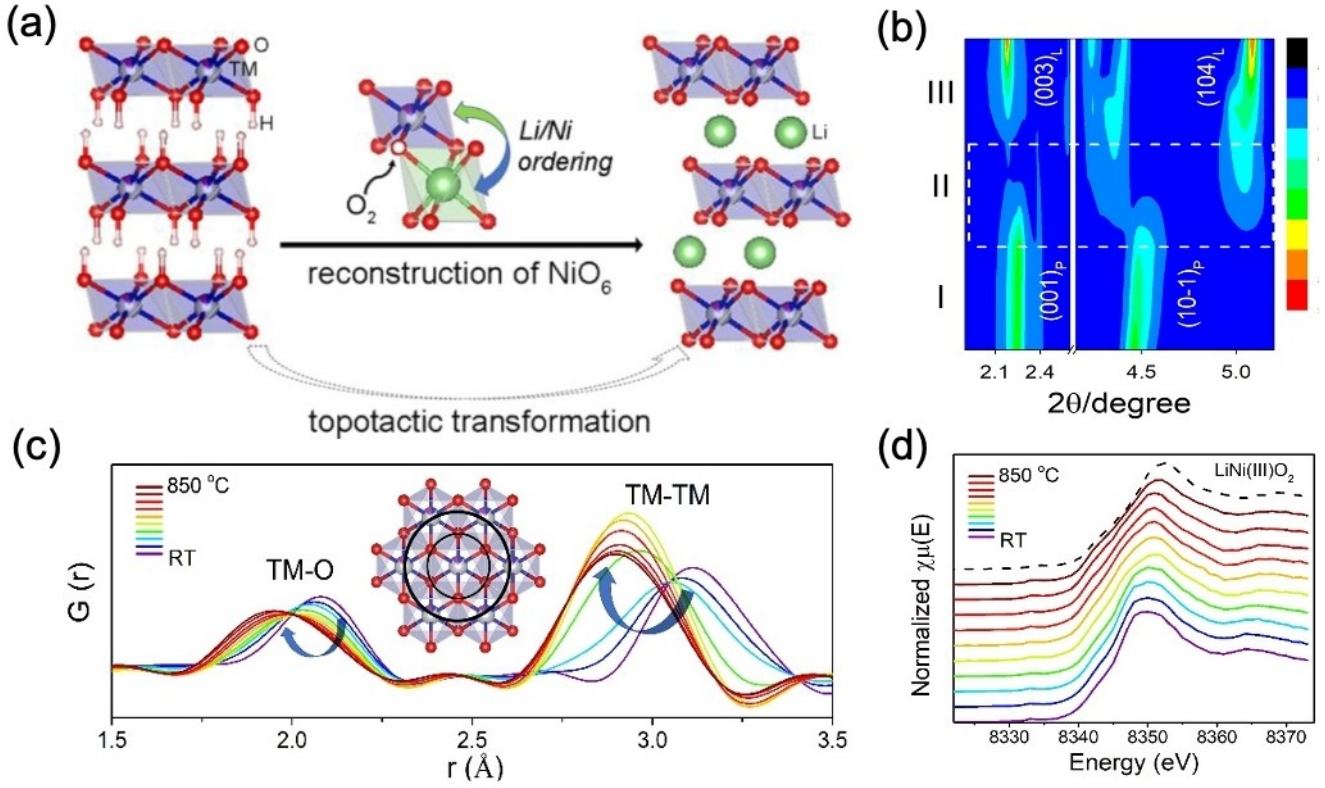

Figure 10. In situ multimodal characterization of the synthesis of NMC771310. a) Schematic of the topotactic transformation from hydroxides to layered oxides, where cationic (dis)ordering is coupled with the reconstruction of basic building units (TMO_6). b–d) Structural/chemical evolution, including long-range/short-range ordering and oxidation of transition metals (Ni, Co, Mn), examined via combined in situ XRD, PDF, and XAS analysis. Adapted with permission from Ref. [45]. Copyright (2018) American Chemical Society.

materials.[49–52] Here, specific examples from recent studies are selected to illustrate the synthesis and processing by design of high-Ni NMC cathodes, in overcoming some of the issues pertaining in such materials.

3. Synthesis and Processing of High-Ni Cathode Materials

3.1. Kinetic Pathways for Formation of Layered Oxides

In situ XRD was employed in studies of synthesis of $LiNiO_2$ and $LiNi_{0.8}Co_{0.2}O_2$ from the acetate precursors, to understand the reaction kinetics and pathways towards ordered layer oxides.[29] The crystal structure of the intermediates and its evolution towards the final product were obtained from the changes in the diffraction patterns, for example, changes in the intensity of (003) reflection, the splitting of (006)/(012) and (018)/(110) doublets, as illustrated in Figure 6(a). More details on structural ordering of layered oxides were obtained by quantifying the evolution of the peak intensity ratio $R = I_{(003)}/I_{(104)}$ (Figure 6b, c), since the reflection from (003) planes is highly sensitive to the ordering while the reflection from (104) planes is independent of the ordering. Rietveld refinement to the in situ XRD data was made to obtain the structural information related to the cationic ordering, such as phase concentration, Li occupancy, local bonding. A direct transformation from rock salt into a layered phase (SG: R-3 m) was revealed, showing that Co substitution facilities the nucleation of a Co-rich layered phase at low temperatures and subsequent growth and stabilization of solid solution $Li(Ni, Co)O_2$ under additional heat treatment (Figure 6d).

Additional structural information, including the Li and Ni(Co) slab distances and their evolution with temperature, was obtained from refinements (Figure 7a). The findings provide important insights into synthetic control of the electrochemical properties of the electrode materials because Li mobility in layered oxides is highly sensitive to the Li slab distance (Figure 7b). For example, the slight change in Li slab distance (i.e., 4%) may cause considerable change in the activation energy for Li immigration (by 200% or higher) and, consequently, a few orders of magnitude reduction in Li diffusivity as predicted by first-principles calculations.[53] Therefore, to enable high electrochemical activity of the layered oxides, precise control of the Li slab distance is needed and may be realized via fine-tuning the synthesis conditions, temperature in particular.

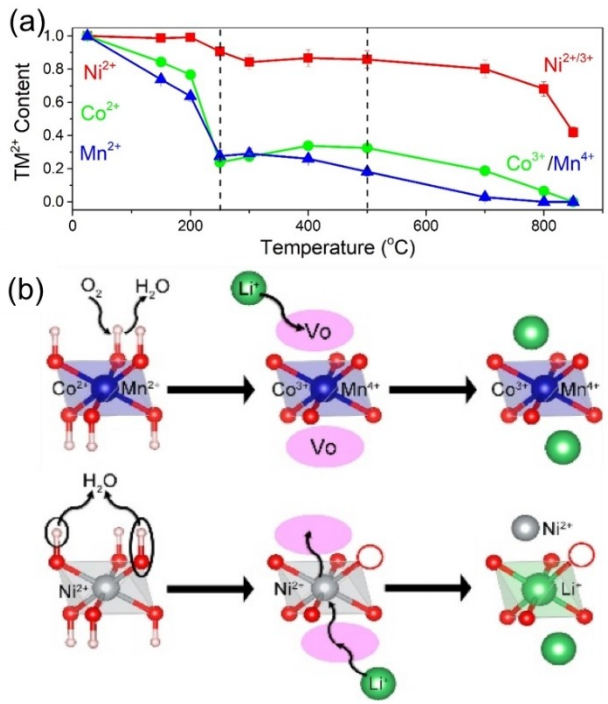

Figure 11. Preferential oxidation of Mn/Co over Ni within basic building units (TMO_6) during synthesis of NMC771310. a) Normalized Ni^{2+}, Co^{2+}, and Mn^{2+} contents as a function of temperature, showing fast oxidation of Co and Mn at low temperatures in contrast to the sluggish oxidation of Ni. b) Schematic of the cationic (dis)ordering coupled with the reconstruction of basic building units from $TM(OH)_6$ to TMO_6, wherein the slow oxidation of Ni leads to oxygen loss and, consequently, the high mobility of Ni (and so the Li/Ni mixing). Adapted with permission from Ref. [45]. Copyright (2018) American Chemical Society.

3.2. Structural Ordering

3.2.1. Kinetics of Cationic Ordering/Disordering

In high-Ni layered oxides, Li/Ni mixing at octahedral sites has been one issue causing low electrochemical activity. In situ synchrotron XRD studies were made to the synthesis of $LiNi_{0.70}Mn_{0.15}Co_{0.15}O_2$ (NMC71515), for understanding and controlling cationic disordering in the system.[54] Information about structural ordering with time and the temperature was obtained directly from the intensity change of the characteristic peak (003) as illustrated in Figure 8(a–c); while more details, such as Li/Ni mixing, were retrieved through quantitative analysis of XRD data (Figure 8d). The in situ observations revealed the competition between cationic ordering and disordering that concomitantly occurred due to Li/O loss during heat treatment. High-temperature treatment is needed to facilitate the ordering process, but the ordering does not increase monotonically with temperature – being compromised by the accelerated disordering as temperature increases. Insights from the in situ studies, specifically on the kinetics of ordering/disordering, provided guidance to synthetic control of the cationic ordering in high-Ni cathodes.[55]

3.2.2. Intrinsic Role of Mn/Co Substitution

Mn/Co substitution has been commonly employed to tune cationic ordering in high-Ni NMC cathodes. In order to better understand the role of Co/Mn substitutions, in situ synchrotron XRD studies were made to the synthesis of a series of layered oxides, $LiNi_{0.7}Mn_xCo_{0.3-x}O_2$ ($0 \leq x \leq 0.3$).[55] The overall ordering process is similar in the 3 different systems, showing an initial improvement followed by deterioration of Li/Ni ordering as they were subjected to heat treatment at 850 °C, as indicated by changes in the intensity ratio of $I_{(003)}/I_{(104)}$. However, the kinetics of the cationic ordering/disordering is much different among the 3 compositions (Figure 9a, b), indicating that Co facilitates Li/Ni ordering; while Mn aggravates Li/Ni mixing and slows down the ordering kinetics. Results from ab initio calculations further confirm the role of Co in reducing the strength of magnetic frustration, strengthening intra-plane super-exchange (SE) interactions. While Mn increases the strength of magnetic frustration and strengthens the inter-plane SE interactions, thereby aggravating Li/Ni mixing, as reflected by the formation energy of the Li/Ni mixing (Figure 9c).

3.2.3. Reconstruction of Basic Building Units

For large-scale industrial applications, NMC layered oxides are mostly synthesized from layered hydroxides (SG: P-3 m1) as precursors, wherein the TM layers comprise edge-sharing TMO_6 and $TM(OH)_6$ octahedra respectively. The overall phase transformation is well known but little is known about local structural change, for example, how the TMO_6 octahedra are inherited from hydroxide precursors through Li/TM re-ordering, subsequently evolving into the layered phase. Through in situ studies using multimodal synchrotron X-ray techniques including XRD, PDF and XAS, the structural/chemical evolution at varying scales down to individual TMO_6 octahedra were obtained during synthesis of $LiNi_{0.77}Mn_{0.13}Co_{0.10}O_2$ (NMC771310) from its hydroxide counterpart (Figure 10).[45] A topotactic transformation throughout the process was revealed and during the process the layered framework was retained (Figure 10a, b). The observation explains the advantage of using hydroxides as precursors for making layered oxides for promoting the structural ordering within the retained framework.

Despite the small structural changes during the topotactic process, significant change occurred locally within the basic octahedral unites, being revealed through in situ total scattering (coupled with PDF analysis) and XAS studies (Figure 10c, d). Particularly, by quantifying the oxidation of individual TM elements, i.e., Ni, Mn and Co, preferential oxidation of Co and Mn over Ni was revealed (Figure 11).[45] Consequently, significant changes within NiO_6 octahedra, including O loss and the associated symmetry breaking. Upon formation of the layered oxides Ni^{2+} ions become highly mobile and tend to mix with Li, which may explain the common observation of high cationic disordering of the initially formed layered phase. Only through

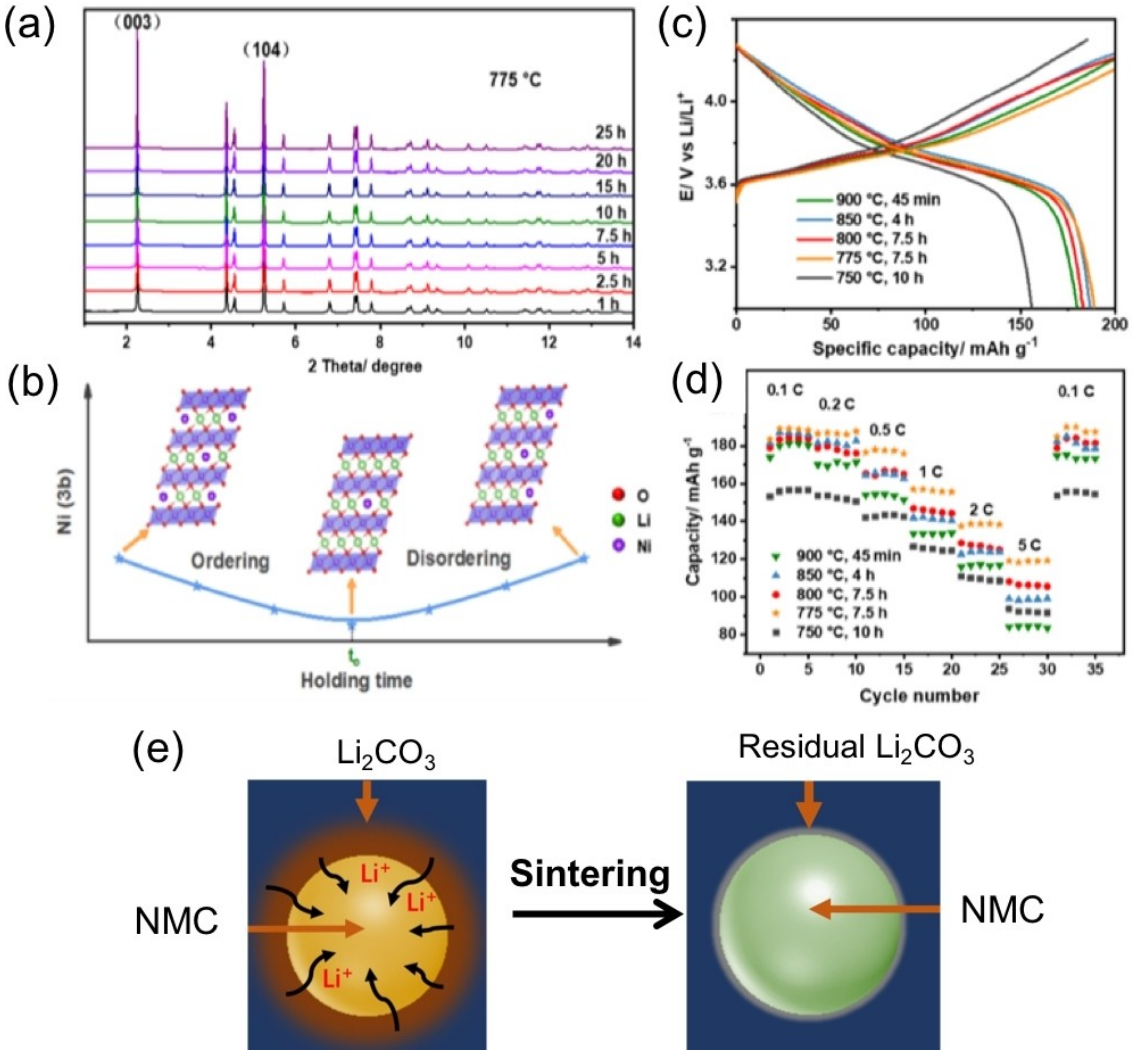

Figure 12. Coupled structural ordering in the bulk and at the surface during sintering and its impact on the electrochemical performance of NMC71515. a) Representative XRD patterns of NMC71515. b) Schematic of cationic ordering/disordering during sintering. c, d) Galvanostatic charge/discharge profiles and rate performances of NMC71515 with optimized structural ordering at different temperatures. e) Schematic of the concurrent structural ordering at the bulk and surface during sintering. Adapted with permission from Ref. [43]. Copyright (2019) Royal Society of Chemistry.

high-temperature heat treatment, Ni was further oxidized, thereby inducing symmetry reconstruction and, concomitantly, cationic ordering within the NiO_6 octahedra. Results from this study provide important insights into synthesis of high-Ni layered oxides, namely, achieving the desired high ordering through efficient oxidation of Ni at the lowest possible temperatures

3.3. Surface Reconstruction

3.3.1. Surface Reconstruction during Synthesis

Synchrotron XRD studies on synthesis of the layered NMC71515 revealed the strong dependence of structural ordering on the sintering conditions (Figure 12a, b).[43] Through tuning the sintering conditions, the ordered NMC71515 was obtained in the temperature range 775–850 °C. Further studies from Galvanostatic cycling experiments (Figure 12c, d) showed that although high capacity was achieved in most of the samples at low rates (except the one synthesized at too low temperature, 750 °C), they showed big difference in the rate capability. According to surface characterization, surface reconstruction occurred besides structural ordering in the bulk, and the sample synthesized at 775 °C exhibited the highest rate capability due to the high structural ordering both in the bulk and surface. Results from this study suggested the concomitant Li/Ni ordering and surface reconstruction, as a result of Li loss from the particle surface during high-temperature sintering (as illustrated in Figure 12e).

3.3.2. Cooling Induced Surface Reconstruction

The surface reconstruction during synthesis can be one critical issue for high-Ni NMC cathodes since the insulating Li_2CO_3 and

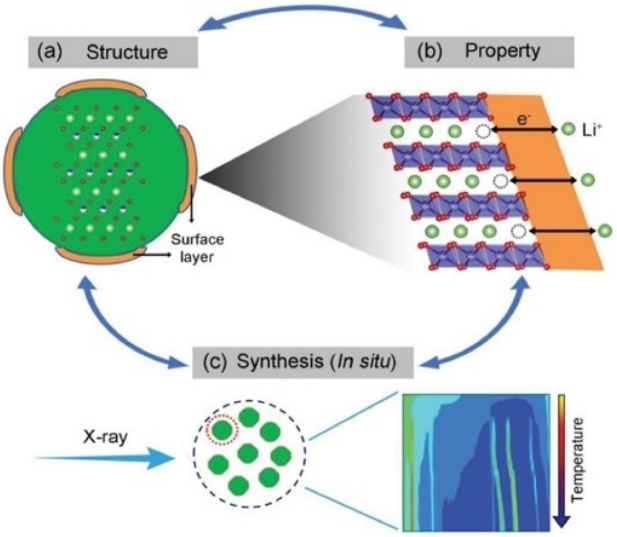

Figure 13. Schematic of the route for developing practically viable high-Ni cathodes *through* a "closed" loop, structure-property-synthesis; specifically, via a) studying the structural reconstruction at surface, b) its impact to electrochemical property, c) the kinetic process and mechanisms using in situ synchrotron X-ray that has high enough detection efficiency to track the formation of minor phases, such as Li_2CO_3 despite its weak scattering of X-ray. Adapted with permission from Ref. [56]. Copyright (2019) Wiley-VCH.

NiO-type rock salt, once formed at the surface, cause impedance to the Li extraction/insertion, as illustrated in Figure 13(a, b). The structural/electrochemical characterization of NMC71515 synthesized at different cooling rates shows the reduced surface reconstruction in samples by quenching and, consequently, the smaller interfacial impedance and higher rate capability compared to the samples by slow cooling.[56] In order to understand how the cooling rate affects the kinetics of cationic ordering and surface reconstruction during synthesis, in situ synchrotron XRD in conjunction with surface analysis was performed to identify all the crystalline phases, not only the main layered phases but also those Li residual species formed at the surface, such as Li_2CO_3 (Figure 13c).

Results from in situ XRD tracking of the whole synthesis process, as presented in Figure 14, reveal that surface reconstruction occurred during the cooling stage, leading to buildup of Li_2CO_3, formation of a Li-deficient layer and reduction of Ni at the particle surface. Such surface reconstruction occurred primarily at high temperatures (above 350 °C), different from the surface reconstruction as observed during storage or electrochemical cycling. The kinetic process is highly cooling rate dependent, and through quenching the reconstruction can be suppressed, thereby improving rate performance. With the revealed origin of surface reconstruction, and demonstrated solutions to alleviate the issue, this work provides guidance to synthesis of high-Ni cathodes, in achieving high structural ordering both in the bulk and surface, for their practical deployment.

4. Perspectives

Significant progress has been made in development and commercialization of high-Ni NMC cathodes for high energy-density LIBs. The NMC oxides with lower Co and even higher Ni content (80% and above) are intensely pursued for further boosting the energy density while reducing the cost of Li-ion cells. On the other hand, the high-Ni loading worsens the surface-instability-related issues, such as capacity-fade during operation and property-degradation during materials production/storage and electrode fabrication, which are becoming the major obstacle to realizing commercial deployment.[15,16] In overcoming those challenges, synthesis and processing will be playing an important role, particularly in tuning the structure, morphology and surface properties of high-Ni cathodes. Some of the new advances in the area, particularly in developing new approaches/strategies, are discussed here.

4.1. Synthetic Control via Manipulating Precursors

The electrochemical performance of high-Ni cathodes is often compromised by their off-stoichiometry and cationic disordering formed during synthesis, which may be tuned by manipulating the low-temperature phases.[57] As illustrated in Figure 15, the synthesis reaction of layered metal oxides proceeded along distinctively different routes when Ni and Co acetates were employed as precursors respectively. The Ni-based layered oxides were topotactically formed from disordered rocksalts ($Li_x(Ni,Co)_{2-x}O_2$; $Fm\bar{3}m$), the intermediate product from acetate-decomposition during low-temperature preheating, and evolved into off-stoichiometric $Li_x(Ni,Co)O_2$ with high Li/Ni mixing. This contrasts with the formation of stoichiometric, ordered $LiCoO_2$, via a spinel intermediate, from the Co-based acetate precursors. This study revealed the importance of the early-stage processing in manipulating the precursors to template the reaction pathways towards targeted structural motifs.

Related studies were reported on synthesis of LCO via $Co(OH)_2$, a layered cobalt hydroxide phase, which provides a lithiation structural template for formation of LCO at much lower temperatures and shortened synthesis time than synthesis from binary oxide precursors.[58] For the similar reason, co-precipitation of layered hydroxides is now the industrially-adopted route towards the synthesis of advanced $Li(Ni_xMn_yCo_z)O_2$ cathode materials.[59] These general principles involving the structure-selection and phase evolution through non-equilibrium intermediates apply beyond layered oxides, as was previously demonstrated in synthesis of $Li_3V_2(PO_4)_3$ (LVP) through a hydrothermal-assisted approach.[50] With the added hydrothermal processing step prior to solid-state synthesis, an amorphous intermediate with local structure resembling that of the final product was obtained, demonstrating the route of manipulating the pathway towards forming nanocrystalline LVP with excellent cycling stability and rate capability.

For synthesis of $Li(Ni_xMn_yCo_z)O_2$ cathode materials, co-precipitation of the hydroxide precursors with intended control

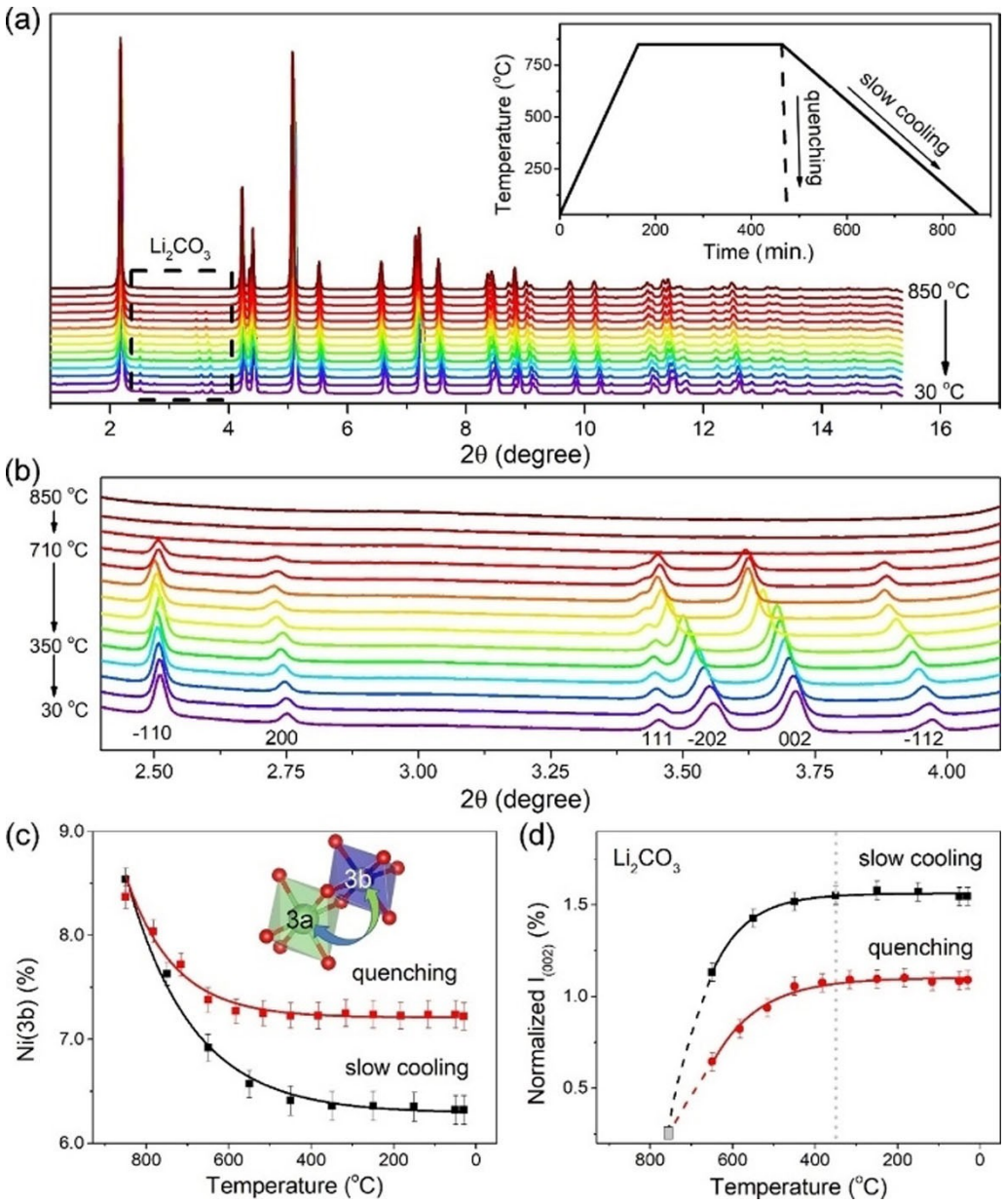

Figure 14. Monitoring the structural ordering and surface reconstruction using in situ synchrotron XRD during synthesis of NMC71515. a) Temperature-resolved in situ XRD for tracking the slow cooling process. Inset: temperature profiles of in situ experiments during slow cooling and quenching (as labeled), using cooling rates of 2 and 200 °C min^{-1}, respectively. b) Zoom-in view of the diffraction patterns associated with Li_2CO_3, as marked by the black dashed square in a). c) The evolution of the percentage of Ni at 3b sites, Ni(3b), as a function of temperature; Inset: schematic of Li/Ni ordering process, showing inter-diffusion of Li/Ni ions between 3a sites (in the TM layers) and 3b sites (in the Li layers). d) The evolution of the integrated area of 002 peak associated with Li_2CO_3 (denoted as I(002), and normalized by I(104) of the layered oxides) as a function of temperature. The dashed lines are extended from the fitting lines and crossed at the gray square, indicating the initial formation of Li_2CO_3 at around 750 °C. No obvious increase of the peak intensity at temperatures below 350 °C (as marked with a dotted line). Adapted with permission from Ref. [56]. Copyright (2019) Wiley-VCH.

of the structure and morphology is crucial to ensure high tap density and minimized surface areas exposed directly to electrolyte. The co-precipitation process is complex, involving a number of reaction parameters (i.e., PH values, type/concentration of salts, temperature) and very few studies have been made on the process.[60] Recent studies, using multiscale simulations in direct comparison to experimental results, provided important insights into the equilibrium and kinetics of coprecipitation reactions and how they are affected by the reaction parameters during the process.[61,62] Through such efforts, in rationalizing the mechanisms driving the formation of non-equilibrium intermediates during synthesis of hydroxide precursors and layered oxides, we may design the early-stage processing or manipulation of the processes towards targeted structural motifs in a more rational way.

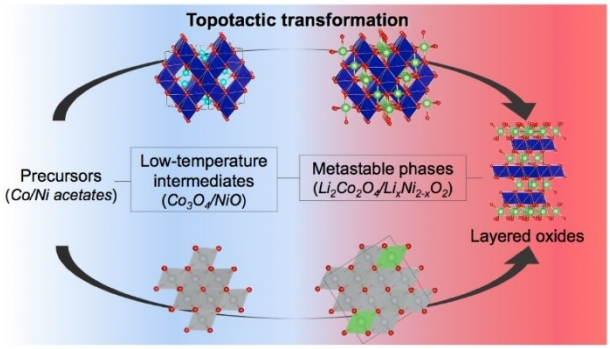

Figure 15. Schematic illustration of the non-equilibrium formation pathways of Co- and Ni-based layered oxides, templated by the low temperature intermediates. Structurally different metal oxides are formed from the decomposition of the Co-based (top) and Ni-based (bottom) acetate salt precursors (as highlighted in blue), and subsequently template the structural-evolution of non-equilibrium intermediates (in red). In the high-temperature calcination process, they all go through a topotactic process before turning into the thermodynamically stable layered phase *(Rm)*. Adapted with permission from Ref. [57]. Copyright (2020) American Chemical Society.

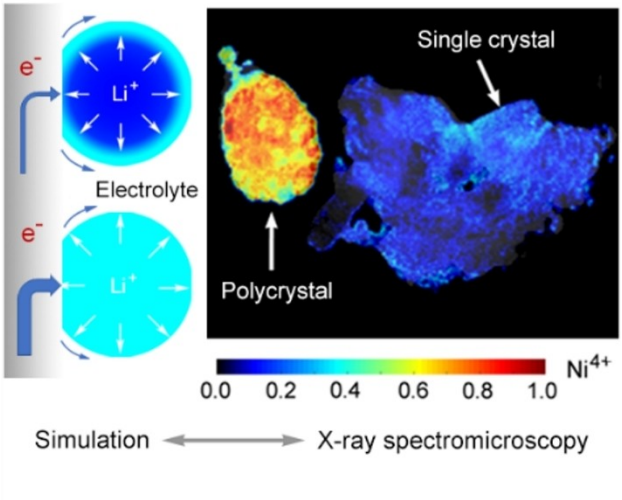

Figure 16. Kinetic limitations in high-Ni cathodes: Sluggish redox kinetics in the single-crystal $LiNi_{0.8}Mn_{0.1}Co_{0.8}O_2$ compared to the polycrystalline revealed by operando X-ray micro-spectroscopy coupled with finite element simulation. Adapted with permission from Ref. [67]. Copyright (2020) Wiley-VCH.

4.2. Morphological Control

Due to the common employment of polycrystalline particles in high-Ni cathodes, the anisotropic volume change and resultant intergranular cracking poses an obstacle to realizing the long cycling stability. Single-crystal NMC cathodes with high Ni content up to 90% exhibit much higher stability compared to their polycrystalline counterparts.[63,64] The replacement with single crystals appears to be promising for eliminating grain boundaries and inter-granular fracture, but the long cycling stability, especially when charging to high voltages, remains to be an issue.[65,66] In addition, surface parasitic reaction may be suppressed in single-crystals due to their smaller specific surface area, but recent studies indicate that the reduced surface-related reaction in single crystals is outweighed by the kinetic limitation, i.e., sluggish Li (de)intercalation in the bulk particularly at the low state of charge (SOC) (Figure 16).[67] For the practical use of high-Ni cathodes, the low Coulombic efficiency particularly during the first cycle is another big concern, but with the mechanistic origins still under debate.[68–70] Both surface reaction and sluggish Li re-intercalation should be responsible, with the latter being found to be dominant in high-Ni NMC cathodes. Control of the particle morphology has been found crucial, but meanwhile challenging in synthesis of high-Ni NMC. For example, synthesizing large-sized single crystals using solid-state reaction requires increasing sintering temperature, which, on the other hand, leads to Li/O loss, formation of rock salt, irregular particle shape, and fracture of the particles. Alternative approaches, such as molten salt or solvothermal synthesis and/or with different types of heating (such as microwave assisted synthesis) may provide solutions by reducing reaction temperature or shortening the reaction time.[71]

4.3. Surface Conditioning

Surface instability is inherent to high-Ni NMC materials and growing evidences show surface reconstruction occurs as they are produced or stored in an ambient environment. Therefore, surface coating is widely employed in industries but mostly through a multiple-step process, which is not only costly but also introduces inconsistency – a major problem for mass production. To realize the commercial potential of the high-Ni cathodes, new processing technologies are needed to solve the inconsistency issue associated with the traditional multi-step process, while lowering cost and reducing wastes/hazards. Many approaches were developed over the years. Notably, a heterogeneous structure construct, such as core-shell or concentration gradient, to improve electrochemical performance, where the high-Ni core delivers high capacity and the low Ni/Mn-rich shell (with relative higher Mn compared to the core region) helps to improve the cyclability and thermal stability.[27] The concept and the derived ones (i.e., with finer compositional control) have been extensively investigated, showing the promise of enhanced energy and lifetime performance compared to homogeneous counterparts. However, implementation of these strategies for large-scale production has been difficult due to the complexity of synthesis in making materials with high compositional heterogeneity. Additional challenge comes from synthetic control of structural ordering particularly when Ni content increases to high values.

In recent efforts, approaches were developed for conditioning both the bulk and surface to stabilize high-Ni NMC.[72,73] It has been demonstrated that Nb coating/doping in NMC 811 was prepared in a one-step heat treatment, with the coating layer to increase the capacity while doping to stabilize the layered structure. As a result, significant improvement was achieved in the 1st capacity loss, discharge capacity, rate performance and cycling stability.[73,74]

The way in which any or all of the developed processes/procedures affect electrode performance is ultimately determined by structural ordering, architecture/morphology, and the surface properties of the cathode materials, which, in turn, are determined during synthesis/processing. With this review on the synthesis/processing-by-design approach and its application to high-Ni cathodes, we demonstrated how the approach may be applied to obtain insights into the reaction pathways, thereby gaining intended control of the structure, morphology and surface properties. Some of the critical issues, such as surface reconstruction, kinetic limitations, mechanical fatigue, thermal stability (among others) pertaining in high-Ni cathodes may be solved or alleviated, paving the way for enabling their practical deployment in next-generation LIBs.

Acknowledgements

We gratefully acknowledge the support of the U.S. Department of Energy, Office of Energy Efficiency and Renewable Energy, Vehicle Technologies Office, under Contract No. DE-SC0012704.

Conflict of Interest

The authors declare no conflict of interest.

Keywords: high-Ni cathodes · in situ characterization · kinetic pathways · lithium-ion batteries · materials synthesis/processing

[1] M. S. Whittingham, *Proc. IEEE* **2012**, *100*, 1518–1534.
[2] B. Dunn, H. Kamath, J.-M. Tarascon, *Science* **2011**, *334*, 928–935.
[3] G. E. Blomgren, *J. Electrochem. Soc.* **2017**, *164*, A5019.
[4] https://energy.gov/sites/prod/files/2014/02/f8/eveverywhere_blueprint.pdf.
[5] D. Andre, S. J. Kim, P. Lamp, S. F. Lux, F. Maglia, O. Paschos, B. Stiaszny, *J. Mater. Chem. A* **2015**, *3*, 6709–6732.
[6] M. S. Whittingham, *Chem. Rev.* **2014**, *114*, 11414–11443.
[7] M. M. Thackeray, S. H. Kang, C. S. Johnson, J. T. Vaughey, R. Benedek, S. A. Hackney, *J. Mater. Chem.* **2007**, *17*, 3112–3125.
[8] J. R. Croy, M. Balasubramanian, K. G. Gallagher, A. K. Burrell, *Acc. Chem. Res.* **2015**, *48*, 2813–2821.
[9] K. Luo, M. R. Roberts, R. Hao, N. Guerrini, D. M. Pickup, Y. S. Liu, K. Edström, J. Guo, A. V. Chadwick, L. C. Duda, P. G. Bruce, *Nat. Chem.* **2016**, *8*, 684–691.
[10] D.-H. Seo, J. Lee, A. Urban, R. Malik, S. Kang, G. Ceder, *Nat. Chem.* **2016**, *8*, 692–697.
[11] G. Assat, J.-M. Tarascon, *Nat. Energy* **2018**, *3*, 373–386.
[12] D. Eum, B. Kim, S. J. Kim, H. Park, J. Wu, S. P. Cho, G. Yoon, M. H. Lee, S. K. Jung, W. Yang, W. M. Seong, *Nat. Mater.* **2020**, *19*, 419–427.
[13] C. Yin, L. Wan, B. Qiu, F. Wang, W. Jiang, H. Cui, J. Bai, S. Ehrlich, Z. Wei, Z. Liu, *Energy Storage Mater.* **2021**, *35*, 388–399.
[14] B. R. Long, J. R. Croy, J. S. Park, J. Wen, D. J. Miller, M. M. Thackeray, *J. Electrochem. Soc.* **2014**, *161*, A2160-A2167.
[15] J. Lee, A. Urban, X. Li, D. Su, G. Hautier, G. Ceder, *Science* **2014**, *343*, 519–522.
[16] J. Lee, D.-H. Seo, M. Balasubramanian, N. Twu, X. Li, G. Ceder, *Energy Environ. Sci.* **2015**, *8*, 3255–3265.
[17] R. Wang, X. Li, L. Liu, J. Lee, D. H. Seo, S. H. Bo, A. Urban, G. Ceder, *Electrochem. Commun.* **2015**, *60*, 70–73.
[18] J. Kim, H. Lee, H. Cha, M. Yoon, M. Park, J. Cho, *Adv. Energy Mater.* **2018**, *8*, 1702028.
[19] A. Manthiram, *Nat. Commun.* **2020**, *11*, 1550.
[20] F. Lin, I. M. Markus, D. Nordlund, T. C. Weng, M. D. Asta, H. L. Xin, M. M. Doeff, *Nat. Commun.* **2014**, *5*, 3529.
[21] J. Zheng, Y. Ye, T. Liu, Y. Xiao, C. Wang, F. Wang, F. Pan, *Acc. Chem. Res.* **2019**, *52*, 2201–2209.
[22] A. O. Kondrakov, A. Schmidt, J. Xu, H. Geßwein, R. Mönig, P. Hartmann, H. Sommer, T. Brezesinski, J. Janek, *J. Phys. Chem. C* **2017**, *121*, 3286–3294.
[23] H.-H. Ryu, K. J. Park, C. S. Yoon, Y. K. Sun, *Chem. Mater.* **2018**, *30*, 1155–1163.
[24] J. Xu, F. Lin, D. Nordlund, E. J. Crumlin, F. Wang, J. Bai, M. M. Doeff, W. Tong, *Chem. Commun.* **2016**, *52*, 4239–4242.
[25] S. E. Renfrew, B. D. McCloskey, *J. Am. Chem. Soc.* **2017**, *139*, 17853–17860.
[26] Y.-K. Sun, S. T. Myung, M. H. Kim, J. Prakash, K. Amine, *J. Am. Chem. Soc.* **2005**, *127*, 13411–13418.
[27] Y.-K. Sun, Z. Chen, H. J. Noh, D. J. Lee, H. G. Jung, Y. Ren, S. Wang, C. S. Yoon, S. T. Myung, K. Amine, *Nat. Mater.* **2012**, *11*, 942–947.
[28] C. P. Grey, D. S. Hall, *Nat. Commun.* **2020**, *11*, 6279.
[29] J. Zhao, W. Zhang, A. Huq, S. T. Misture, B. Zhang, S. Guo, L. Wu, Y. Zhu, Z. Chen, K. Amine, F. Pan, J. Bai, F. Wang, *Adv. Energy Mater.* **2016**, *7*, 1601266.
[30] H. H. Sun, H. H. Ryu, U. H. Kim, J. A. Weeks, A. Heller, Y. K. Sun, C. B. Mullins, *ACS Energy Lett.* **2020**, *5*, 1136–1146.
[31] J. Cabana, B. J. Kwon, L. Hu, *Acc. Chem. Res.* **2018**, *51*, 299–303.
[32] J. Bai, J. Hong, H. Chen, J. Graetz, F. Wang, *J. Phys. Chem. C* **2015**, *119*, 2266–2276.
[33] J. Chen, J. Bai, H. Chen, J. Graetz, *J. Phys. Chem. Lett.* **2011**, *2*, 1874–1878.
[34] Z. Chen, Y. Ren, Y. Qin, H. Wu, S. Ma, J. Ren, X. He, Y. K. Sun, K. Amine, *J. Mater. Chem.* **2011**, *21*, 5604–5609.
[35] H. M. Rietveld, *J. Appl. Crystallogr.* **1969**, 2, 65–71.
[36] R. O. Jones, O. Gunnarsson, *Rev. Mod. Phys.* **1989**, *61*, 689.
[37] Y.-C. K. Chen-Wiegart, S. Campbell, K. G. Yager, Y. Liu, A. Frenkel, L. Yang, J. Bai, M. McCormick, D. Allan, M. Basham, "Multi-modal Synchrotron Characterization: Modern Techniques and Data Analysis" in *Handbook on Big Data and Machine Learning in the Physical Sciences*, Vol. 1 (Eds.: S. Kalidindi, S. V. Kalinin, T. Lookman, I. Foster), World Scientific, Singapore, **2020**, pp. 39–64.
[38] X. Li, X. Ma, D. Su, L. Liu, R. Chisnell, S. P. Ong, H. Chen, A. Toumar, J. C. Idrobo, Y. Lei, J. Bai, F. Wang, J. W. Lynn, Y. S. Lee, G. Ceder, *Nat. Mater.* **2014**, *13*, 586–592.
[39] Y. U. Park, J. Bai, L. Wang, G. Yoon, W. Zhang, H. Kim, S. Lee, S. W. Kim, J. P. Looney, K. Kang, F. Wang, *J. Am. Chem. Soc.* **2017**, *139*, 12504–2516.
[40] T. Threlfall, *Org. Process Res. Dev.* **2003**, *7*, 1017–1027.
[41] M. Avrami, *J. Chem. Phys.* **1941**, *9*, 177–184.
[42] S. A. Arrhenius, *J. Phys. Chem.* **1889**, *4*, 96–116.
[43] Y. Duan, L. Yang, M. J. Zhang, Z. Chen, J. Bai, K. Amine, F. Pan, F. Wang, *J. Mater. Chem. A* **2019**, *7*, 513–519.
[44] H. Jonsson, G. Mills, K. W. Jacobson in *Classical and quantum dynamics in condensed phase simulations*, Chap. 16 (Eds.: B. J. Berne, G. Ciccotti, D. F. Coker), World Scientific, Singapore, **1998**, pp. 385–404.
[45] M.-J. Zhang, G. Teng, Y. C. K. Chen-Wiegart, Y. Duan, J. Y. P. Ko, J. Zheng, J. Thieme, E. Dooryhee, Z. Chen, J. Bai, K. Amine, F. Pan, F. Wang, *J. Am. Chem. Soc.* **2018**, *140*, 12484–12492.
[46] I. D. Brown, *Chem. Rev.* **2009**, *109*, 6858–6919.
[47] J. Liu, P. S. Whitfield, M. R. Saccomanno, S. H. Bo, E. Hu, X. Yu, J. Bai, C. P. Grey, X. Q. Yang, P. G. Khalifah, *J. Am. Chem. Soc.* **2017**, *139*, 9192–9202.
[48] M. Bianchini, J. Wang, R. J. Clément, B. Ouyang, P. Xiao, D. Kitchaev, T. Shi, Y. Zhang, Y. Wang, H. Kim, M. Zhang, J. Bai, F. Wang, W. Sun, G. Ceder, *Nat. Mater.* **2020**, *19*, 1088–1095.
[49] D. P. Shoemaker, Y–J. Hu, D. Chung, G. J. Halder, P. J. Chupas, *Proc. Natl. Acad. Sci. USA* **2014**, *111*, 10922–10927.
[50] L. Wang, J. Bai, P. Gao, X. Wang, J. P. Looney, F. Wang, *Chem. Mater.* **2015**, *27*, 5712–5718.
[51] B.-R. Chen, W. Sun, D. A. Kitchaev, J. S. Mangum, V. Thampy, L. M. Garten, D. S. Ginley, B. P. Gorman, K. H. Stone, G. Ceder, M. F. Toney, *Nat. Commun.* **2018**, *9*, 2553.
[52] Y. Li, R. Xu, Y. Ren, J. Lu, H. Wu, L. Wang, D. J. Miller, Y. K. Sun, K. Amine, Z. Chen, *Nano Energy* **2016**, *19*, 522–531.
[53] K. Kang, G. Ceder, *Phys. Rev. B* **2006**, *74*, 094105.

[54] D. Wang, R. Kou, Y. Ren, C. J. Sun, H. Zhao, M. J. Zhang, Y. Li, A. Huq, J. P. Ko, F. Pan, Y. K. Sun, Y. Yang, K. Amine, J. Bai, Z. Chen, F. Wang, *Adv. Mater.* **2017**, *29*, 1606715.
[55] D. Wang, C. Xin, M. Zhang, J. Bai, J. Zheng, R. Kou, J. Y. P. Ko, A. Huq, G. Zhong, C. J. Sun, Y. Yang, Z. Chen, X. Xiao, K. Amine, F. Pan, F. Wamg, *Chem. Mater.* **2019**, 31, 2731–2740.
[56] M. Zhang, X. Hu, M. Li, Y. Duan, L. Yang, C. Yin, M. Ge, X. Xiao, W.-K. Lee, J. Y. P. Ko, K. Amine, Z. Chen, Y. Zhu, E. Dooryhee, J. Bai, F. Pan, F. Wang, *Adv. Energy Mater.* **2019**, 91901915.
[57] J. Bai, W. Sun, J. Zhao, D. Wang, P. Xiao, J. Y. P. Ko, A. Huq, G. Ceder, F. Wang, *Chem. Mater.* **2020**, *32*, 9906–9913.
[58] B. Huang, Y. I. Jang, Y. M. Chiang, D. R. Sadoway, *J. Appl. Electrochem.* **1998**, *28*, 1365–1369.
[59] Y.-J. Shin, W. J. Choi, Y. S. Hong, S. Yoon, K. S. Ryu, S. H. Chang, *Solid State Ionics* **2006**, *177*, 515–521.
[60] A. V. Bommel, J. R. Dahn, *Chem. Mater.* **2009**, *21*, 1500–1503.
[61] F. Zhang, P. Barai, J. Gim, K. Yuan, Y. A. Wu, Y. Xie, Y. Liu, V. Srinivasan, *J. Electrochem. Soc.* **2018**, *165*, A3077-A3083.
[62] P. Barai, Z. Feng, H. Kondo, V. Srinivasan, *J. Phys. Chem. B* **2019**, *123*, 3291–3303.
[63] J. Li, A. R. Cameron, H. Li, S. Glazier, D. Xiong, M. Chatzidakis, J. Allen, G. A. Botton, J. R. Dahn, *J. Electrochem. Soc.* **2017**, *164*, A1534-A1544.
[64] X. Fan, G. Hu, B. Zhang, X. Ou, J. Zhang, W. Zhao, H. Jia, L. Zou, P. Li, Y. Yang, *Nano Energy* **2020**, *70*, 104450.
[65] G. Qian, Y. Zhang, L. Li, R. Zhang, J. Xu, Z. Cheng, S. Xie, H. Wang, Q. Rao, Y. He, Y. Shen, Z. Ma, *Energy Storage Mater.* **2020**, *27*, 140–149.
[66] Y. Bi, J. Tao, Y. Wu, L. Li, Y. Xu, E. Hu, B. Wu, J. Hu, C. Wang, J. G. Zhang, Y. Qi, J. Xiao, *Science* **2020**, *370*, 1313–1317.
[67] M. Ge, S. Wi, X. Liu, J. Bai, S. Ehrlich, D. Lu, W.-K. Lee, Z. Chen, F. Wang, *Angew. Chem. Int. Ed.* **2021**, *60*, 17350.
[68] J. Kasnatscheew, M. Evertz, B. Streipert, R. Wagner, R. Klöpsch, B. Vortmann, H. Hahn, S. Nowak, M. Amereller, A.-C. Gentschev, P. Lamp, M. Winter, *Phys. Chem. Chem. Phys.* **2016**, *18*, 3956–3965.
[69] H. Zhou, F. X. Xin, B. Pei, M. S. Whittingham, *ACS Energy Lett.* **2019**, *4*, 1902–1906.
[70] A. Grenier, P. J. Reeves, H. Liu, I. D. Seymour, K. Marker, K. M. Wiaderek, P. J. Chupas, C. P. Grey, K. W. Chapman, *J. Am. Chem. Soc.* **2020**, *142*, 7001–7011.
[71] M. Zhang, Y. Duan, C. Yin, M. Li, H. Zhong, E. Dooryhee, K. Xu, F. Pan, F. Wang, J. Bai, *Sci. Adv.* **2020**, *6*, eabd9472.
[72] F. Schipper, H. Bouzaglo, M. Dixit, E. M. Erickson, T. Weigel, M. Talianker, J. Grinblat, L. Burstein, M. Schmidt, J. Lampert, C. Erk, B. Markovsky, D. T. Major, D. Aurbach, *Adv. Energy Mater.* **2018**, *8*, 1701682.
[73] F. Xin, H. Zhou, X. Chen, M. Zuba, N. Chernova, G. Zhou, M. S. Whittingham, *ACS Appl. Mater. Interfaces* **2019**, *11*, 34889–34894.
[74] F. Xin, H. Zhou, Y. Zong, M. Zuba, Y. Chen, N. A. Chernova, J. Bai, B. Pei, A. Goel, J. Rana, F. Wang, K. An, L. F. J. Piper, G. Zhou, M. S. Whittingham, *ACS Energy Lett.* **2021**, *6*, 1377.

Manuscript received: July 20, 2021
Accepted manuscript online: July 27, 2021
Version of record online: August 19, 2021